

# Chlorodifluoroacetyl Azide, $\text{ClF}_2\text{CC}(\text{O})\text{N}_3$ : Preparation, Properties, and Decomposition

Luis A. Ramos,<sup>†</sup> Xiaoqing Zeng,<sup>§</sup> Sonia E. Ulic,<sup>†,‡</sup> Helmut Beckers,<sup>§</sup> Helge Willner,<sup>§</sup> and Carlos O. Della Védova<sup>\*,†,||</sup>

<sup>†</sup>CEQUINOR (UNLP-CONICET), Departamento de Química, Facultad de Ciencias Exactas, Universidad Nacional de La Plata, 47 esq. 115, 1900 La Plata, Argentina

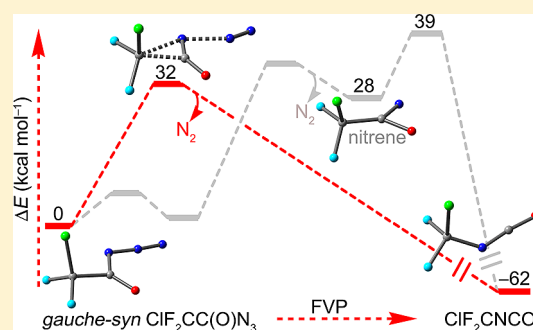
<sup>‡</sup>Departamento de Ciencias Básicas, Universidad Nacional de Luján, Rutas 5 y 7 (6700), Luján, Argentina

<sup>§</sup>Fachbereich C - Anorganische Chemie, Bergische Universität Wuppertal, 42097 Wuppertal, Germany

<sup>||</sup>Laboratorio de Servicios a la Industria y al Sistema Científico (UNLP-CIC-CONICET), Buenos Aires, Argentina

## Supporting Information

**ABSTRACT:** Chlorodifluoroacetyl azide,  $\text{ClF}_2\text{CC}(\text{O})\text{N}_3$ , was prepared and characterized by IR (gas, Ar matrix), Raman (liquid), UV-vis (gas), and  $^{19}\text{F}$ ,  $^{13}\text{C}$  NMR spectroscopy. The vibrational spectra were analyzed in terms of a single conformer, *gauche-syn*, where the Cl-C and the  $\text{N}_\alpha=\text{N}_\beta$  bonds are *gauche* and *syn* to the C=O bond, respectively. The photo and thermal decomposition reactions of the azide were studied with the aid of matrix isolation. In both cases, a new isocyanate species  $\text{ClF}_2\text{CNCO}$  was produced and characterized by matrix IR spectroscopy. The conformational properties and the Curtius rearrangement pathways of this new carbonyl azide were theoretically explored, which suggest the preference of a concerted over stepwise decomposition for the global minimum *gauche-syn* conformer.



## INTRODUCTION

Covalent azides are well-known for their potential shock, thermal, and photolytic sensitivity, and consequently, they have been classified as explosives or high energy materials. Compared to the rather sensitive inorganic azides, organic azides are relatively easier to handle and some of them have been widely used as synthetic reagents in organic and biological chemistry.<sup>1</sup> Carbonyl azides ( $\text{RC}(\text{O})\text{N}_3$ ) are versatile precursors for producing isocyanates ( $\text{RNCO}$ ) through the well-known Curtius rearrangement.<sup>2</sup> Their synthesis, reactivity, and physical properties have been extensively studied both theoretically and experimentally.

Perhaps the best known carbonyl azide is benzoyl azide,  $\text{PhC}(\text{O})\text{N}_3$ , which can be easily prepared and safely handled.<sup>3</sup> Its decomposition reactions have been studied for several decades.<sup>4</sup> Following the early attempts to obtain  $\text{N}_3\text{C}(\text{O})\text{C}(\text{O})\text{N}_3$ ,<sup>5</sup> metastable simple carbonyl azides  $\text{CH}_3\text{C}(\text{O})\text{N}_3$ <sup>6</sup> and  $\text{CF}_3\text{C}(\text{O})\text{N}_3$ <sup>7</sup> were merely generated as in situ reagents, and their spectroscopic and structural properties remain unknown still. Recently, the extremely explosive carbonyl diazide,  $\text{N}_3\text{C}(\text{O})\text{N}_3$ , was isolated as a neat substance and structurally characterized.<sup>8</sup> The elusive parent compound  $\text{HC}(\text{O})\text{N}_3$  has been only very recently prepared in solution and spectroscopically characterized; however, no isolation could be achieved due to its facile decomposition at ambient conditions.<sup>9</sup> One of the most interesting reactions of carbonyl azides,  $\text{RC}(\text{O})\text{N}_3$ , is the generation of the highly reactive carbonyl nitrene intermediate,

$\text{RC}(\text{O})\text{N}$ , by extruding molecular nitrogen upon photolysis or pyrolysis,<sup>1</sup> the nitrene may easily isomerize to the corresponding isocyanate,  $\text{RNCO}$  through Curtius rearrangement. However, study of the intermediates involved in the decomposition of carbonyl azides continues to be of interest.<sup>10</sup>

In view of the rich chemistry of carbonyl azides, we report herein the first synthesis of chlorodifluoroacetyl azide,  $\text{ClF}_2\text{CC}(\text{O})\text{N}_3$ . The conformational properties of this compound were investigated using vibrational (IR, Raman) spectroscopy as guided by quantum chemical calculations. Its photochemical and thermal decompositions to a new isocyanate compound  $\text{ClF}_2\text{CNCO}$  were studied using matrix isolation IR spectroscopy. The involved Curtius rearrangement mechanism was theoretically explored using DFT calculations.

## RESULTS AND DISCUSSION

**General Properties.** Solid chlorodifluoroacetyl azide,  $\text{ClF}_2\text{CC}(\text{O})\text{N}_3$ , melts at  $-64\text{ }^\circ\text{C}$  to a colorless liquid. For safety reasons, the vapor pressure of the liquid was determined only at  $-1\text{ }^\circ\text{C}$  (24.2 mbar).

The  $^{19}\text{F}$  NMR spectrum of the liquid shows one singlet at  $\delta = -65.7$  ppm attributed to the fluorine atoms of the  $\text{CClF}_2$  group; the  $^{13}\text{C}$  NMR spectrum exhibits two triplet signals centered at  $\delta = 166.1$  ppm ( $^2J_{(\text{C}-\text{F})} = 34.4$  Hz) and  $\delta = 117.2$

Received: May 11, 2012

Published: July 16, 2012

ppm ( $^1J_{\text{C-F}} = 299.3$  Hz), corresponding to the carbon atoms of the C=O and CClF<sub>2</sub> groups, respectively (Figure S1, Supporting Information). The chemical shifts are close to those reported for similar compounds.<sup>11,12</sup>

The UV-vis spectrum of gaseous ClF<sub>2</sub>CC(O)N<sub>3</sub> (Figure S2, Supporting Information) shows two absorption bands with  $\lambda_{\text{max}} = 228$  and 192 nm similar to those of other carbonyl azides. These features are assigned to the  $n \rightarrow \pi^*$  and  $\pi \rightarrow \pi^*$  transitions, respectively.<sup>8</sup>

**Calculated Conformers and Relative Energies.** The conformational properties of ClF<sub>2</sub>CC(O)N<sub>3</sub> were explored by locating the minimum energy structures on the potential energy curves around the C(1)–C(2) and C(2)–N(1) bonds by using the B3LYP/6-311+G(d) method (Figure 1). Four low energy

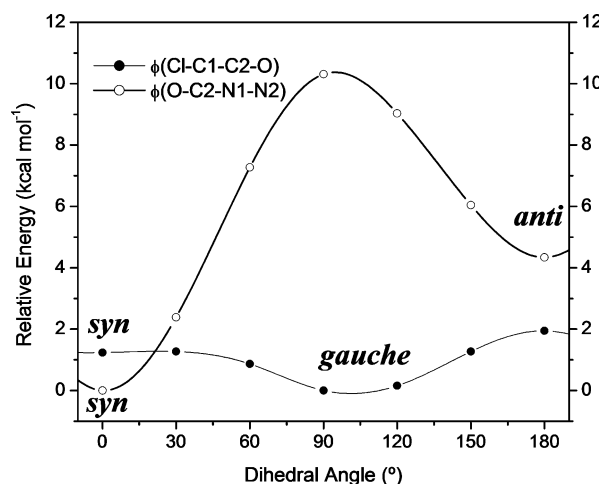


**Figure 1.** Calculated potential energy curves for the internal rotation around the C1–C2 and C2–N1 bonds of ClF<sub>2</sub>CC(O)N<sub>3</sub> by using the B3LYP/6-311+G(d) method. The relax scan of the potential energy surface was performed by rotating the dihedral angle, either Cl–C1–C2–O or O–C2–N1–N2, in steps of 30° while optimizing the rest of the molecule.

conformers, *gauche-syn*, *gauche-anti*, *syn-syn* and *syn-anti*, depicted in Figure 2, were found on the potential energy surface. Full structural optimizations for these molecules were performed using DFT (B3LYP) and ab initio (MP2) methods with 6-311+G(d) and 6-311+G(3df) basis sets, and the CBS-QB3 method was also applied. The calculated relative energies, standard Gibbs free energy differences, and the Boltzmann

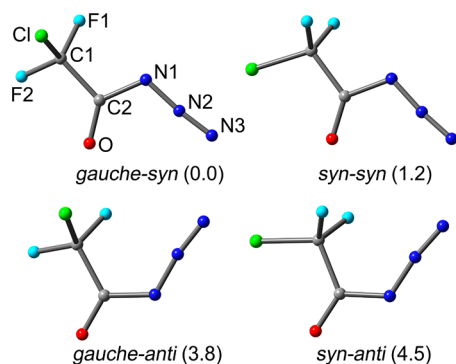


**Figure 2.** Optimized structures with atomic labeling and relative energies (kcal mol<sup>-1</sup>) for the minimum energy conformations of ClF<sub>2</sub>CC(O)N<sub>3</sub> at the B3LYP/6-311+G(3df) level of theory.

distributions of the four conformers at room temperature are listed in Table 1.

For the lowest energy *gauche-syn* form, the C(1)–C(2) bond is *gauche* ( $\phi(\text{Cl}-\text{C}(1)-\text{C}(2)-\text{O}) = 102^\circ$ ) to the C=O double bond, while the N(1)=N(2) bond is *syn* ( $\phi(\text{O}-\text{C}(2)-\text{N}(1)-\text{N}(2)) = 0^\circ$ ) to the same group. This *gauche-syn* conformer was predicted by all methods to be the most abundant form in the gas phase with an estimated contribution of 64% based on the CBS-QB3 calculated Gibbs free energy difference ( $\Delta G$ ) at room temperature. The higher energy *syn-syn* form is predicted to make a contribution of 36%, while the other two have negligible contributions. The predicted distribution of conformers varies somewhat between calculation models, but all three predict *gauche-syn* and *syn-syn* to be present in observable quantities.

An interesting result is the rather shallow rotational energy barrier ( $<1$  kcal mol<sup>-1</sup>, B3LYP/6-311+G(d)) around the C(1)–C(2) bond in ClF<sub>2</sub>CC(O)N<sub>3</sub> (Figure 1), which should allow an easy rotational interconversion of the higher energy *syn-syn* conformer to the *gauche-syn* form. This feature, which is consistent with the measured vibrational spectra, will be discussed in connection with the matrix experiments (see below). In contrast, ClF<sub>2</sub>CC(O)N<sub>3</sub> has much larger rotational energy barrier ( $\sim 5$  kcal mol<sup>-1</sup>, B3LYP/6-311+G(d)) for the conversion from the higher energy *anti* conformer to the *syn* around the C(2)–N(1) bond, and the energy difference  $\Delta E^\circ$  between them is more than 4 kcal mol<sup>-1</sup>. This barrier (Figure 1) and large Gibbs free energy differences (Table 1) to the most stable *gauche-syn* conformer suggest neither the *gauche-anti* nor *syn-anti* form is likely to be detected at room temperature, a conclusion also consistent with the experimental results discussed below.

**Vibrational Spectra.** IR spectra of ClF<sub>2</sub>CC(O)N<sub>3</sub> (gas phase and Ar matrix) and the Raman spectrum of the liquid were recorded; the results are shown in Figure 3. The observed band positions are listed in Table 2 and compared with the calculated frequencies for the two lowest energy conformers.

According to the theoretical calculations (Table 1), the *syn-syn* conformer of ClF<sub>2</sub>CC(O)N<sub>3</sub> is expected to be in equilibrium with the global minimum *gauche-syn* form. However, given the bandwidths of observed IR and Raman spectra and the calculated frequency differences ( $\Delta\nu$ ) for these two rotamers, no conclusive evidence for the presence of a second rotamer could be obtained.

Matrix-isolation IR spectroscopy is a well-known technique for studying conformational equilibria.<sup>13</sup> The IR fundamentals of Ar-matrix-isolated ClF<sub>2</sub>CC(O)N<sub>3</sub> (1:2000) show weak satellite bands within a few wavenumbers, which are attributed to matrix effects rather than the presence of the *syn-syn* conformer, as evidenced by the disparity between the experimental and calculated  $\Delta\nu$  in Table 2. The matrix IR spectrum indicates that the lowest energy *gauche-syn* conformer is the only form present in the matrix. However, the very low energy barrier ( $<1$  kcal mol<sup>-1</sup>, Figure 1) for the *syn-syn*  $\rightarrow$  *gauche-syn* interconversion makes it likely that the *syn-syn* form, if present in the gas phase, may isomerize to the lowest energy *gauche-syn* conformer during the deposition process. The conformational composition of the gas-phase remains unchanged during the cooling process only if the barrier exceeds 3 kcal mol<sup>-1</sup>,<sup>14</sup> a value which is substantially higher than that calculated for the *syn-syn*  $\rightarrow$  *gauche-syn* interconversion of ClF<sub>2</sub>CC(O)N<sub>3</sub> (Figure 1).

**Table 1.** Calculated Relative Total Energies ( $\Delta E$ , kcal mol<sup>-1</sup>), Gibbs Free Energies ( $\Delta G$ , kcal mol<sup>-1</sup>) for the Conformers of ClF<sub>2</sub>CC(O)N<sub>3</sub> and Their Predicted Population<sup>a</sup> in the Gas Phase at 298 K

| method             | gauche-syn       |                  |    | syn-syn          |                  |    | gauche-anti      |                  |   | syn-anti         |                  |   |
|--------------------|------------------|------------------|----|------------------|------------------|----|------------------|------------------|---|------------------|------------------|---|
|                    | $\Delta E^\circ$ | $\Delta G^\circ$ | %  | $\Delta E^\circ$ | $\Delta G^\circ$ | %  | $\Delta E^\circ$ | $\Delta G^\circ$ | % | $\Delta E^\circ$ | $\Delta G^\circ$ | % |
| B3LYP/6-311+G(d)   | 0.00             | 0.00             | 74 | 1.20             | 0.21             | 26 | 4.22             | 4.58             | 0 | 4.92             | 5.17             | 0 |
| B3LYP/6-311+G(3df) | 0.00             | 0.00             | 84 | 1.15             | 0.57             | 16 | 3.78             | 4.17             | 0 | 4.47             | 4.77             | 0 |
| CBS-QB3            | 0.00             | 0.00             | 64 | 0.93             | -0.08            | 36 | 3.45             | 3.84             | 0 | 3.94             | 4.26             | 0 |

<sup>a</sup>Degeneracies of the forms are taken into account.

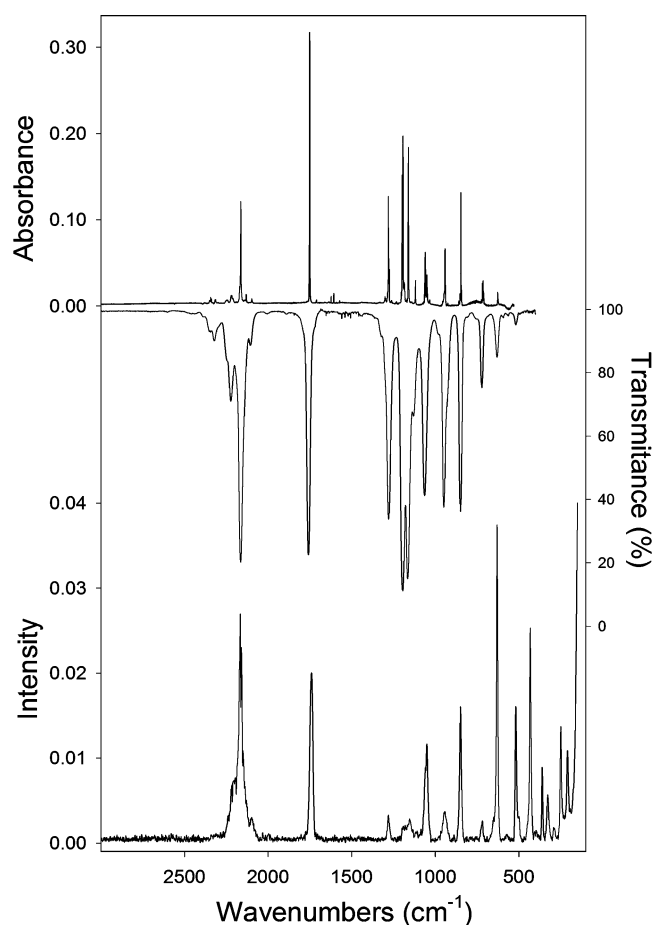


**Figure 3.** Upper trace: IR spectrum of ClF<sub>2</sub>CC(O)N<sub>3</sub> isolated in solid Ar at 15 K (resolution: 0.25 cm<sup>-1</sup>). Middle trace: IR spectrum of gaseous ClF<sub>2</sub>CC(O)N<sub>3</sub> at 298 K (resolution: 2 cm<sup>-1</sup>). Lower trace: Raman spectrum of liquid ClF<sub>2</sub>CC(O)N<sub>3</sub> at 298 K (resolution: 2 cm<sup>-1</sup>).

All 21 fundamental vibrational modes of the ClF<sub>2</sub>CC(O)N<sub>3</sub> molecule are expected to be active in both the IR and Raman spectra. The antisymmetric and symmetric stretching modes of the azide group (N<sub>3</sub>) were observed at 2164 and 1279 cm<sup>-1</sup>, respectively, as strong and medium-strong bands in the IR spectrum of the gas. The IR band at 1759 cm<sup>-1</sup> and Raman band at 1740 cm<sup>-1</sup> are assigned to the  $\nu$ (C=O) fundamental in keeping the calculated frequency (1801 cm<sup>-1</sup>, *gauche-syn*) and also by comparison with the data reported for similar molecules, such as F<sub>3</sub>CC(O)NCO (1795 and 1785 cm<sup>-1</sup>)<sup>15</sup> and N<sub>3</sub>C(O)N<sub>3</sub> (1756 and 1721 cm<sup>-1</sup>).<sup>8</sup> The intense IR band at 1195 cm<sup>-1</sup> is assigned to the C(1)–C(2) stretching mode on the basis of the IR frequencies reported for similar molecules.<sup>11</sup> The three IR bands at 1165, 1064, and 949 cm<sup>-1</sup> are attributed to the stretching modes of the CClF<sub>2</sub> group by comparison

with the values calculated for the *gauche-syn* conformer at 1164, 1064, and 934 cm<sup>-1</sup>, respectively.

The strongest band in the Raman spectrum of the liquid is at 631 cm<sup>-1</sup> and is identified as the characteristic CF<sub>2</sub> deformation mode (coupled with  $\nu$ (C–Cl) vibration). This frequency is close to the same mode observed in ClF<sub>2</sub>CC(O)SH<sup>11</sup> at 639 cm<sup>-1</sup>. The N<sub>3</sub> deformation in ClF<sub>2</sub>CC(O)N<sub>3</sub> is attributed to the medium-strong scattering at 518 cm<sup>-1</sup>, and it is close to that in FC(O)N<sub>3</sub> at 565 cm<sup>-1</sup>.<sup>16</sup> In addition, what is substantially the  $\nu$ (C–Cl) fundamental of ClF<sub>2</sub>CC(O)N<sub>3</sub> is attributed to the intense Raman band at 432 cm<sup>-1</sup>, which is without an obvious IR counterpart. The calculated <sup>35</sup>Cl/<sup>37</sup>Cl isotopic shift is less than 1 cm<sup>-1</sup> (B3LYP/6-311+G(3df)) and consequently could not be observed. The Raman bands at wavenumbers below 400 cm<sup>-1</sup> correspond mainly to deformation and torsional vibrations, as described in Table 2.

**Photolysis and Pyrolysis.** The UV spectrum of gaseous ClF<sub>2</sub>CC(O)N<sub>3</sub> shows two intense absorptions at 192 and 228 nm (Figure S2, Supporting Information), which invite the performance of irradiation studies. The IR difference spectrum showing the spectral changes after  $\lambda > 225$  nm photolysis of Ar-matrix isolated ClF<sub>2</sub>CC(O)N<sub>3</sub> is given in Figure 4 (lower trace). After 10 min of UV–vis broad band photolysis, virtually complete depletion of the IR bands of ClF<sub>2</sub>CC(O)N<sub>3</sub> was observed, together with the simultaneous appearance of a few new bands. The assignments are collected in Table 3, while a complete list of all the new bands which develop on photolysis is given in Table S1 in the Supporting Information.

Among the new IR bands, the most intense one occurs at 2282.3 cm<sup>-1</sup>, which is assigned to the antisymmetric stretch of the NCO group ( $\nu_{as}$ (NCO)) of the expected Curtius-rearrangement product ClF<sub>2</sub>CNCO after nitrogen loss from the azide precursor. The symmetric stretch ( $\nu_s$ (NCO)) appears at 1463.0 cm<sup>-1</sup> as a much weaker band. The other weak absorptions observed at 1150.5, 1116.0, and 1001.7 cm<sup>-1</sup> can be assigned to the vibrational modes of the CClF<sub>2</sub> group. The assignments are supported by the calculation of the low energy *gauche* conformer of ClF<sub>2</sub>CNCO (Table 3). No clear IR bands were found for the possible nitrene intermediate. The exclusive formation of isocyanate ClF<sub>2</sub>CNCO from the photolytic decomposition of ClF<sub>2</sub>CC(O)N<sub>3</sub> is consistent with the previous observations that the carbonyl nitrene intermediates are photosensitive to UV–visible irradiations. For example, the recently observed triplet nitrene FC(O)N evolves rapidly to FNCO under UV radiation.<sup>10b</sup>

Photolysis of matrix-isolated ClF<sub>2</sub>CC(O)N<sub>3</sub> was also performed using an ArF excimer laser (193 nm). Similarly, the decomposition product ClF<sub>2</sub>CNCO was found. Some additional very weak IR bands were observed after the laser photolysis, which could be associated with the elusive nitrene intermediate; however, no positive conclusion could be drawn due to the rather low abundance of the carrier in the matrix.

**Table 2. Experimental and Calculated Frequencies ( $\text{cm}^{-1}$ ) and Assignments of the Fundamental Vibrational Modes of  $\text{ClF}_2\text{CC}(\text{O})\text{N}_3$** 

| mode       | experimental          |                               |                             | calculated <sup>d</sup> |                  | assignment <sup>e</sup>                           |
|------------|-----------------------|-------------------------------|-----------------------------|-------------------------|------------------|---|
|            | IR (gas) <sup>a</sup> | IR (Ar matrix) <sup>b,c</sup> | Raman (liquid) <sup>c</sup> | <i>gauche-syn</i>       | <i>syn-syn</i>   |   |
| $\nu_1$    | 2164 s                | 2164.4 (51)                   | 2167/2160 (72)              | 2295 (448)[113]         | 2295 (437) [106] | $\nu_{\text{as}}(\text{N}_3)$                     |
| $\nu_2$    | 1759 s                | 1752.0 (52)                   | 1740 (53)                   | 1801 (257)[18]          | 1804 (201)[13]   | $\nu(\text{C}=\text{O})$                          |
| $\nu_3$    | 1279 ms               | 1280.8 (30)                   | 1282 (8)                    | 1304 (439)[<1]          | 1296 (504)[<1]   | $\nu_s(\text{N}_3)$                               |
| $\nu_4$    | 1195 s                | 1193.4 (100)                  | 1185 (4)                    | 1235 (138)[4]           | 1205 (74)[6]     | $\nu(\text{C}-\text{C})$                          |
| $\nu_5$    | 1165 ms               | 1160.6 (48)                   | 1151 (7)                    | 1164 (168)[1]           | 1110 (186)[2]    | $\nu_{\text{as}}(\text{CF}_2)$                    |
| $\nu_6$    | 1064 m                | 1060.6 (35)                   | 1059/1050 (30)              | 1063 (248) [13]         | 1094 (104) [10]  | $\nu_s(\text{CF}_2)$ , $\nu(\text{C}-\text{N})$   |
| $\nu_7$    | 949 m                 | 943.3 (30)                    | 945 (10)                    | 934 (134) [4]           | 922 (254) [6]    | $\nu(\text{CCl})$ , $\nu_s(\text{CCN})$           |
| $\nu_8$    | 849 m                 | 847.1 (21)                    | 849 (42)                    | 851 (115) [6]           | 850 (237) [3]    | $\nu(\text{CCl}) + \delta(\text{CNN})$            |
| $\nu_9$    | 721 mw                | 714.5 (8)                     | 718 (7)                     | 722 (55) [2]            | 756 (18) [<1]    | $\gamma(\text{CC}(\text{O})\text{N})$             |
| $\nu_{10}$ | 625 mw                | 627.8 (5)                     | 631 (100)                   | 625 (33) [8]            | 662 (3) [9]      | $\delta(\text{CF}_2)$ , $\nu(\text{C}-\text{Cl})$ |
| $\nu_{11}$ |                       |                               |                             | 586 (<1) [1]            | 591 (4) [<1]     | $\delta_{\text{oop}}(\text{N}_3)$                 |
| $\nu_{12}$ | 518 w                 |                               | 518 (42)                    | 534 (6) [5]             | 533 (3) [5]      | $\delta(\text{N}_3)$                              |
| $\nu_{13}$ |                       |                               | 498 (7)                     | 500 (4) [1]             | 380 (1) [5]      | $\rho(\text{CF}_2)$                               |
| $\nu_{14}$ |                       |                               | 432 (67)                    | 421 (<1) [5]            | 439 (<1) [2]     | $\nu(\text{C}-\text{Cl})$ , $\delta(\text{CF}_2)$ |
| $\nu_{15}$ |                       |                               | 360 (32)                    | 356 (1) [1]             | 416 (<1) [1]     | $\rho(\text{CO})$ , $\delta(\text{CF}_2)$         |
| $\nu_{16}$ |                       |                               | 327 (15)                    | 323 (<1) [1]            | 264 (2) [3]      | $\delta_{\text{twist}}(\text{CF}_2)$              |
| $\nu_{17}$ |                       |                               | 249 (37)                    | 245 (3) [2]             | 282 (<1) [<1]    | $\delta_{\text{wag}}(\text{CF}_2)$                |
| $\nu_{18}$ |                       |                               | 209 (28)                    | 199 (1) [1]             | 225 (5) [2]      | $\gamma(\text{O}-\text{C}-\text{N}-\text{N})$     |
| $\nu_{19}$ |                       |                               |                             | 133 (<1) [4]            | 121 (<1) [4]     | $\rho(\text{CClF}_2)$                             |
| $\nu_{20}$ |                       |                               |                             | 84 (<1) [4]             | 89 (<1) [3]      | $\tau((\text{O})\text{C}-\text{N}_3)$             |
| $\nu_{21}$ |                       |                               |                             | 40 (<1) [1]             | 13 (2) [<1]      | $\tau(\text{CClF}_2-\text{C}(\text{O}))$          |

<sup>a</sup>Relative band intensities: s, strong; ms, medium strong; mw, medium weak; w, weak. <sup>b</sup>Only the most populated Ar-matrix sites are given. <sup>c</sup>Relative intensities based on the integration of band areas are given in parentheses. <sup>d</sup>B3LYP/6-311+G(3df) calculated frequencies ( $\text{cm}^{-1}$ ), IR intensities in parentheses ( $\text{km mol}^{-1}$ ), and Raman intensities ( $\text{\AA}^4 \text{amu}^{-1}$ ) in square brackets. <sup>e</sup> $\nu$ ,  $\delta$ ,  $\rho$  and  $\tau$  represent stretching, deformation, rocking and torsion modes, respectively.

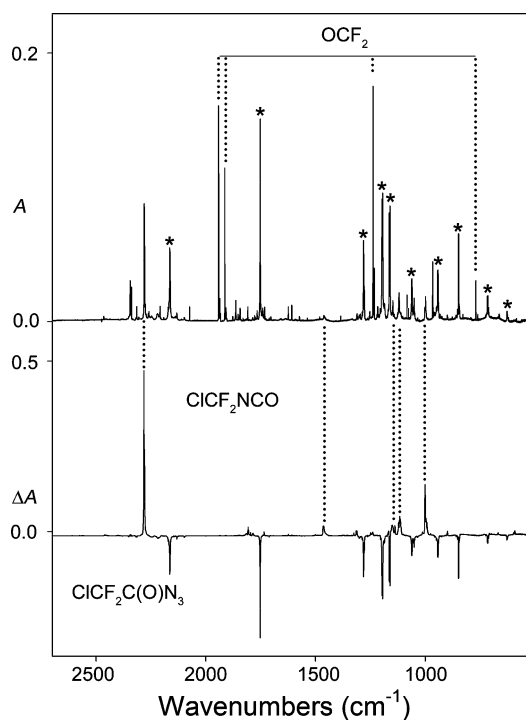


**Figure 4.** Upper trace: IR spectrum of matrix-isolated pyrolysis (280 °C) products of  $\text{ClF}_2\text{CC}(\text{O})\text{N}_3$ ; the bands of the azide are marked by asterisks. Lower trace: IR difference spectrum recorded before and after 10 min of UV-vis irradiation ( $\lambda > 225 \text{ nm}$ ) of Ar-matrix isolated  $\text{ClF}_2\text{CC}(\text{O})\text{N}_3$ . The IR bands of newly formed species point upward while those of depleted  $\text{ClF}_2\text{CC}(\text{O})\text{N}_3$  point downward.

Flash vacuum pyrolysis (FVP) of argon-diluted  $\text{ClF}_2\text{CC}(\text{O})\text{N}_3$  at 280 °C was performed by passing the mixture through a hot nozzle which was heated by a 10 mm platinum wire before deposition onto the matrix. The decomposition products were quenched as matrix, the IR spectrum of which is shown in Figure 4 (upper trace). The decomposition of the azide was indicated by the appearance of a number of new IR bands. Some of these coincide with the bands previously assigned to the aforementioned  $\text{ClF}_2\text{CNCO}$ .

The IR spectrum of the matrix-isolated pyrolysis products includes strong bands at 1941.4, 1913.4, 1237, and 965.4  $\text{cm}^{-1}$ . These match, respectively, the  $\nu(\text{CO})$ ,  $2\nu_s(\text{CF}_2)$ ,  $\nu_{\text{as}}(\text{CF}_2)$ , and  $\nu_s(\text{CF}_2)$  vibrational modes of  $\text{OCF}_2$ .<sup>17</sup> On the assumption of a unimolecular decomposition process and taking into account the high matrix dilution (1:2000), the formation of  $\text{OCF}_2$  requires the simultaneous evolution of  $\text{ClCN}$  following the elimination of  $\text{N}_2$  from  $\text{ClF}_2\text{CC}(\text{O})\text{N}_3$ . In fact, weak but distinct IR bands observed at 2208.6 and 717.7  $\text{cm}^{-1}$  can be attributed to the  $\nu(\text{CN})$  and  $\nu(\text{ClC})$  fundamentals of  $\text{ClCN}$ . These frequencies are in good agreement with the values reported for an authentic sample (2208.6 and 717.8  $\text{cm}^{-1}$ ) in the Ar matrix.<sup>18</sup>

**Calculated Curtius Rearrangement.** The potential energy surface (PES) for the Curtius rearrangement of the global minimum conformer of  $\text{ClF}_2\text{CC}(\text{O})\text{N}_3$  (*gauche-syn*) was calculated using the B3LYP/6-311+G(3df) calculations. Two distinct pathways from the lowest energy *gauche-syn* conformer to  $\text{ClF}_2\text{CNCO}$  were found. The results are depicted in Figure 5. The energetically more favorable path is a concerted way of losing  $\text{N}_2$  with simultaneous formation of  $\text{ClF}_2\text{CNCO}$ , which corresponds to a calculated barrier of 31.9  $\text{kcal mol}^{-1}$  (TS1). In contrast, the higher energy route comprises a first conforma-

**Table 3.** Observed Band Positions ( $\text{cm}^{-1}$ ), Relative Intensities, and Assignments for the IR Bands of the Ar-Matrix Isolated Pyrolysis (280 °C) and Photolysis ( $\lambda > 225 \text{ nm}$ , 10 min) Products of  $\text{ClF}_2\text{CC}(\text{O})\text{N}_3$  at 15 K

| IR (Ar matrix)                          |   | species                   | assignment                       | ref                      |
|---|---|---------------------------|----------------------------------|--------------------------|
| pyrolysis                               | photolysis                              |                           |                                  |                          |
| $\nu$ ( $\text{cm}^{-1}$ ) <sup>a</sup> | $\nu$ ( $\text{cm}^{-1}$ ) <sup>a</sup> |                           |                                  |                          |
| 2280.7 (100)                            | 2282.3 (100)                            | $\text{ClF}_2\text{CNCO}$ | $\nu_{\text{as}}(\text{NCO})$    | 2359 (1139) <sup>b</sup> |
| 2208.6 (2)                              |   | $\text{ClCN}$             | $\nu(\text{CN})$                 | 2208.6 <sup>c</sup>      |
| 1941.4/1935.7 (56)                      |   | $\text{OCF}_2$            | $\nu(\text{CO})$                 | 1941 <sup>d</sup>        |
| 1913.4/1906.8 (41)                      |   | $\text{OCF}_2$            | $2(\nu_s(\text{CF}_2))$          | 1913 <sup>d</sup>        |
| 1460.3 (7)                              | 1463.0 (14)                             | $\text{ClF}_2\text{CNCO}$ | $\nu_s(\text{NCO})$              | 1501 (172) <sup>b</sup>  |
| 1237.7/1231.2 (67)                      |   | $\text{OCF}_2$            | $\nu_{\text{as}}(\text{CF}_2)$   | 1239 <sup>d</sup>        |
| 1146.8 (11)                             | 1150.5 (19)                             | $\text{ClF}_2\text{CNCO}$ | $\nu_{\text{as}}(\text{CClF}_2)$ | 1156 (337) <sup>b</sup>  |
| 1118.9 (<1)                             | 1116.0 (<1)                             | $\text{ClF}_2\text{CNCO}$ | $\nu_s(\text{CClF}_2)$           | 1101 (297) <sup>b</sup>  |
| 998.0 (26)                              | 1001.7/995.7 (39)                       | $\text{ClF}_2\text{CNCO}$ | $\nu_{\text{as}}(\text{CClF}_2)$ | 965 (412) <sup>b</sup>   |
| 965.4/960.6 (15)                        |   | $\text{OCF}_2$            | $\nu_s(\text{CF}_2)$             | 966 <sup>d</sup>         |
| 769.0/759.3 (8)                         |   | $\text{OCF}_2$            | $\delta(\text{FCO})$             | 764 <sup>d</sup>         |
|   | 707.1 (1)                               | $\text{ClF}_2\text{CNCO}$ | $\delta \text{CF}_2$             | 720 (38) <sup>b</sup>    |
|   | 667.5 (1)                               | $\text{ClF}_2\text{CNCO}$ | $\delta(\text{NCO})$             | 670 (16) <sup>b</sup>    |
|   | 595.1 (1)                               | $\text{ClF}_2\text{CNCO}$ | $\delta(\text{NCO})$             | 613 (24) <sup>b</sup>    |

<sup>a</sup>Relative intensities based on the integration of band areas are given in parentheses. <sup>b</sup>Calculated vibrational frequencies ( $\text{cm}^{-1}$ ) and absolute intensities ( $\text{km mol}^{-1}$ ) in parentheses at the B3LYP/6-311+(3df) level of theory. <sup>c</sup>Reference 18. <sup>d</sup>Reference 17.

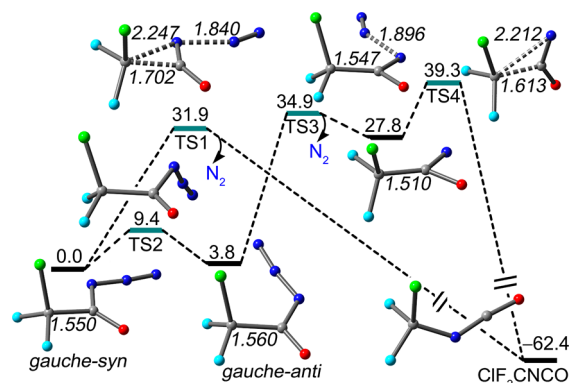


**Figure 5.** Calculated potential energy surface for stepwise and concerted Curtius rearrangement of *gauche-syn*  $\text{ClF}_2\text{CC}(\text{O})\text{N}_3$  at the B3LYP/6-311+G(3df) level of theory. The relative energies are given in  $\text{kcal mol}^{-1}$  and selective bond lengths (italics) given in Å.

tional conversion of the *syn* azide to *anti* with an activation barrier of  $9.4 \text{ kcal mol}^{-1}$  (TS2); then the latter decomposes into the nitrene intermediate with a significant barrier of  $31.1 \text{ kcal mol}^{-1}$  (TS3), eventually the singlet nitrene rearranges to  $\text{ClF}_2\text{CNCO}$  with a moderate barrier of  $11.5 \text{ kcal mol}^{-1}$  (TS4). The higher overall barrier of the stepwise rearrangement route suggests that the thermal decomposition of the azide will mostly occur through a concerted way without passing by the nitrene intermediate. In contrast, photolytic dissociation of the azide may happen via both ways due to the large excess of energy input upon irradiation, where the azide in the excited state may also be involved under the photolysis conditions.

The preference of a concerted decomposition pathway has also been suggested based on calculations for other carbonyl azides like  $\text{CH}_3\text{C}(\text{O})\text{N}_3$ <sup>4c</sup> and  $\text{HC}(\text{O})\text{N}_3$ .<sup>9</sup> As far as we know, no nitrene intermediate but mostly Curtius rearrangement product has been obtained during the thermal decomposition of carbonyl azide. For all of these carbonyl azides, the lower energy *syn* conformer of the azide prefers a concerted decomposition due to the steric effect; i.e., the substituent in the *syn* conformer ( $\text{ClF}_2\text{C}$  in  $\text{ClF}_2\text{CC}(\text{O})\text{N}_3$ ) may easily

approach the  $\alpha$ -nitrogen atom of the azide group, as a result a three-membered ring is formed and the  $\text{N}_\alpha\text{-N}_\beta$  bond is elongated (TS1 in  $\text{ClF}_2\text{CC}(\text{O})\text{N}_3$ ). However, in the *anti* conformer, such approach is hindered by the steric repulsion between the substituent and the azide group ( $\text{ClF}_2\text{C}$  in  $\text{ClF}_2\text{CC}(\text{O})\text{N}_3$ ). As a compensation, the stabilizing intramolecular  $\text{N}_\alpha\cdots\text{O}$  interaction in singlet carbonyl nitrenes may facilitate the formation of an oxazirone-like intermediate by reducing the  $\text{O-C-N}_\alpha$  angle ( $\angle\text{OCN}_\alpha = 89.9^\circ$  in  $\text{ClF}_2\text{CC}(\text{O})\text{N}$ ). Nonetheless, the rather small energy gap between singlet and triplet  $\text{ClF}_2\text{CC}(\text{O})\text{N}$  ( $0.8 \text{ kcal mol}^{-1}$ , CBS-QB3) indicates the possible occurrence of rapid intersystem crossing (ISC) between the two electronic states. Such a low energy gap (ca.  $4.0 \text{ kcal mol}^{-1}$ ) has been experimentally inferred for a closely related carbonyl nitrene  $\text{F}_3\text{CC}(\text{O})\text{N}$ , for which the calculated  $\Delta E_{\text{S-T}}$  was found to be dependent on the calculation method used.<sup>19</sup>

## CONCLUSIONS

The new high energy chlorodifluoroacetyl azide ( $\text{ClF}_2\text{CC}(\text{O})\text{N}_3$ ) has been synthesized and characterized. Quantum chemical calculations predict four minimum energy conformers for the azide and the coexistence of the *gauche-syn* and *syn-syn* forms in the gas phase at room temperature. In practice, however, only the lowest energy *gauche-syn* rotamer was observed when the vapor was trapped in a solid Ar matrix. It is assumed that the very small rotational barrier ( $<1 \text{ kcal mol}^{-1}$ ) calculated at the B3LYP/6-311+G(d) level of approximation for the *syn-syn*  $\rightarrow$  *gauche-syn* conformational conversion causes this change to occur spontaneously during quenching of the diluted sample onto the cold matrix support.

UV photolysis ( $\lambda > 225 \text{ nm}$  and  $\lambda = 193 \text{ nm}$ ) of  $\text{ClF}_2\text{CC}(\text{O})\text{N}_3$  isolated in a solid Ar matrix leads via the loss of  $\text{N}_2$  to a new isocyanate  $\text{ClF}_2\text{CNCO}$  formed through the Curtius rearrangement. Pyrolysis of the azide at  $280 \text{ }^\circ\text{C}$  also produces  $\text{ClF}_2\text{CNCO}$  together with  $\text{OCF}_2$  and  $\text{ClCN}$ . DFT calculations on the Curtius rearrangement of  $\text{ClF}_2\text{CC}(\text{O})\text{N}_3$  explain the absence of any nitrene intermediate during the thermal decomposition of the azide which reacts in a concerted

manner. The photolytic decomposition gives rise to some unknown weak IR features which might be associated with the nitrene, further experiments to generate and characterize this elusive intermediate are currently underway.

## ■ EXPERIMENTAL SECTION

**Caution!** Covalent azides are explosive. Although no explosions were encountered with  $\text{ClF}_2\text{CC}(\text{O})\text{N}_3$  during this work, it should be handled with care in millimolar quantities, and appropriate safety precautions should be taken, especially when working with the liquid or solid  $\text{ClF}_2\text{CC}(\text{O})\text{N}_3$ .

**Synthesis.** Chlorodifluoroacetyl azide,  $\text{ClF}_2\text{CC}(\text{O})\text{N}_3$ , was synthesized by the reaction of chlorodifluoroacetyl chloride,  $\text{ClF}_2\text{CC}(\text{O})\text{Cl}$ , and sodium azide,  $\text{NaN}_3$ . For this purpose,  $\text{ClF}_2\text{CC}(\text{O})\text{Cl}$  (0.3 g, 2.0 mmol) was distilled into a glass vessel provided with a vacuum valve and containing dried  $\text{NaN}_3$  (0.5 g, 7.7 mmol).<sup>20</sup> The reaction vessel was then placed in a metallic container for protection. The reaction was complete after 3 h at room temperature. Volatile products were collected and separated by repeated fractional condensation using traps held at  $-70$ ,  $-95$ , and  $-196$  °C. The product (0.22 g, 1.4 mmol),  $\text{ClF}_2\text{CC}(\text{O})\text{N}_3$ , was retained in the first trap together with a small amount of unreacted  $\text{ClF}_2\text{CC}(\text{O})\text{Cl}$  from which it could be freed by slow vacuum evaporation. The quality of the samples was checked by reference to the IR spectrum of the vapor and to the  $^{19}\text{F}$  and  $^{13}\text{C}$  NMR spectra of the liquid. The final yield was around 70% based on  $\text{ClF}_2\text{CC}(\text{O})\text{Cl}$ . The starting material,  $\text{ClF}_2\text{CC}(\text{O})\text{Cl}$ , was prepared by chlorination of the corresponding acid,  $\text{ClF}_2\text{CC}(\text{O})\text{OH}$  (98%), with  $\text{PCl}_5$  (>98%).<sup>21</sup>  $\text{NaN}_3$  was a commercial reagent.

**Instrumentation and Procedure.** (a) *General Procedure.* Volatile materials were manipulated in a glass vacuum line equipped with a capacitance pressure gauge, three U-traps, and valves with PTFE stems. The vacuum line was connected to an IR cell (optical path length 200 mm, Si windows 0.5 mm thick) placed in the sample compartment of a FTIR spectrometer. This arrangement made it possible to follow the course of the preparative reaction and the purification processes. The pure compound was stored in flame-sealed glass ampules under liquid nitrogen in a Dewar vessel. Each ampule could be opened with an ampule key<sup>22</sup> at the vacuum line, an appropriate amount was withdrawn for the experiments, and the ampule was then flame-sealed again. The vapor pressure of a sample was measured in a small vacuum line equipped with a calibrated capacitance pressure gauge and a small sample reservoir. The melting point was determined using a small amount of the sample contained in a 4 mm glass tube immersed in a cold bath in a transparent Dewar vessel; the temperature was increased at a rate of about  $1.0$  °C  $\text{min}^{-1}$  starting at  $-90$  °C (cold ethanol bath).

(b) *Vibrational Spectroscopy.* Infrared spectra of gaseous samples were recorded at a resolution of  $2$   $\text{cm}^{-1}$  in the range from  $4000$  to  $400$   $\text{cm}^{-1}$ , using a glass cell with Si windows and an optical path length of 200 mm. Raman spectra of the neat liquid in a flame-sealed capillary (3 mm o.d.) at room temperature in the region from  $4000$  to  $100$   $\text{cm}^{-1}$  at a resolution of  $2$   $\text{cm}^{-1}$ .

(c) *Matrix Isolation Experiments.* For matrix isolation experiments,  $\text{ClF}_2\text{CC}(\text{O})\text{N}_3$  was diluted with argon in the proportions 1:2000 in a 1 L stainless-steel storage container. Small amounts of the mixture were deposited within 10 min on the cold matrix support (15 K, Rh-plated Cu block) in a high vacuum. Temperature-dependent experiments were carried out by passing the gaseous sample-Ar mixtures through a quartz nozzle (1 mm i.d.), heated over a length of  $\sim 10$  mm with a platinum wire (0.25 mm o.d.) prior to deposition on the matrix support. The nozzle was held at  $110$  or  $280$  °C. Photolysis experiments were performed using an ArF excimer laser (193 nm) with a total exposure time of 7 min (2.5 mJ, 5 Hz repetition time) or with a high-pressure mercury lamp using a cutoff filter giving radiation with  $\lambda > 225$  nm (10 min).

IR spectra of matrix isolated samples were recorded in a reflectance mode on a spectrometer using a transfer optic. An MCT detector and a KBr/Ge beam splitter were used in the spectral range of  $5000$ – $530$   $\text{cm}^{-1}$ . For the spectra with apodized resolutions of  $0.25$   $\text{cm}^{-1}$ , 200

scans were added. More details of the matrix apparatus are given elsewhere.<sup>23</sup>

(d) *UV Spectroscopy.* The UV–vis spectrum of gaseous  $\text{ClF}_2\text{CC}(\text{O})\text{N}_3$  was recorded using a glass cell equipped with quartz windows (100 mm optical path length). Measurements were carried out in the spectral region from  $190$  to  $700$  nm with a sampling interval of  $1.0$  nm, a scan speed of  $200$   $\text{nm min}^{-1}$  and a slit width of  $2$  nm.

(e) *NMR Spectroscopy.* For  $^{13}\text{C}$  (100.6 MHz) and  $^{19}\text{F}$  (376.5 MHz) NMR spectra, a pure sample of liquid  $\text{ClF}_2\text{CC}(\text{O})\text{N}_3$  was flame-sealed in a thin-walled 4 mm o.d. tube which was placed inside a 5 mm NMR tube. The sample was held at  $-20$  °C, and  $\text{CDCl}_3$  was used as an external lock and reference.

(f) *Theoretical Calculations.* Quantum chemical calculations were performed using a commercial program package.<sup>24</sup> Scans of the potential energy surface, structure optimizations, and calculations of vibrational frequencies for  $\text{ClF}_2\text{CC}(\text{O})\text{N}_3$  were carried out by applying density functional theory (B3LYP)<sup>25</sup> and complete basis set CBS-QB3 methods.<sup>26</sup> 6-311+G(d) and 6-311+G(3df) basis sets were employed.

## ■ ASSOCIATED CONTENT

### ■ Supporting Information

Vibrational frequencies and assignments of IR bands observed for the products trapped in an Ar matrix following pyrolysis ( $280$  °C) and photolysis ( $\lambda > 225$  nm) of  $\text{ClF}_2\text{CC}(\text{O})\text{N}_3$ ;  $^{19}\text{F}$  and  $^{13}\text{C}$  NMR and UV–visible spectra of  $\text{ClF}_2\text{CC}(\text{O})\text{N}_3$ ; and calculated energies and atomic coordinates for all optimized structures at the B3LYP/6-311+G(3df) level of theory. This material is available free of charge via the Internet at <http://pubs.acs.org>.

## ■ AUTHOR INFORMATION

### ■ Corresponding Author

\*E-mail: [carlosdv@quimica.unlp.edu.ar](mailto:carlosdv@quimica.unlp.edu.ar).

### ■ Notes

The authors declare no competing financial interest.

## ■ ACKNOWLEDGMENTS

We thank the Deutscher Akademischer Austauschdienst Germany (DAAD), Agencia Nacional de Promoción Científica y Técnica (ANPCYT), Consejo Nacional de Investigaciones Científicas y Técnicas (CONICET), Comisión de Investigaciones de la Provincia de Buenos Aires (CIC), Facultad de Ciencias Exactas, Universidad Nacional de La Plata (UNLP), and Departamento de Ciencias Básicas de la Universidad Nacional de Luján for financial support. L.A.R. gratefully acknowledges the DAAD, UNLP, and Bergische Universität Wuppertal. S.E.U. thanks the Deutscher Akademischer Austauschdienst Germany (DAAD) for an equipment grant and financial support. C.O.D.V. acknowledges the DAAD, which generously sponsors the DAAD Regional Program of Chemistry for Argentina supporting Latin American students to carry out Ph.D. research in La Plata. X.Z., H.B., and H.W. acknowledge the support of the Deutsche Forschungsgemeinschaft.

## ■ REFERENCES

- (1) See, for examples: (a) Platz, M. S. In *Reactive Intermediates*; Moss, R. A., Platz, M. S., Jones, M. J., Eds.; Wiley-Interscience: 2004. (b) *Azides and Nitrenes; Reactivity and Utility*; Scriven, E. F. V., Ed.; Academic Press Inc.: New York, 1984.
- (2) Curtius, T. *Ber. Dtsch. Chem. Ges.* **1890**, *23*, 3023–3041.
- (3) Bhaskar, K. R. *Indian J. Chem. Eng* **1966**, *4*, 368.
- (4) See, recent examples: (a) Vyas, S.; Kubicki, J.; Luk, H. L.; Zhang, Y.; Gritsan, N. P.; Hadad, C. M.; Platz, M. S. *J. Phys. Org. Chem.* **2012**, *25*, 693–703. (b) Wentrup, C.; Bornemann, H. *Eur. J. Org. Chem.*

- 2005, 4521–4524. (c) Liu, J.; Mandel, S.; Hadad, C. M.; Platz, M. S. *J. Org. Chem.* **2004**, *69*, 8583–8593. (d) Pritchina, E. A.; Gritsan, N. P.; Maltsev, A.; Bally, T.; Autrey, T.; Liu, Y.; Wang, Y.; Toscano, J. P. *Phys. Chem. Chem. Phys.* **2003**, *5*, 1010–1018.
- (5) Roesky, H.; Glemser, O. *Chem. Ber.* **1964**, *97*, 1710–1712.
- (6) Frankel, M. B.; Woolery, D. O. *J. Org. Chem.* **1983**, *48*, 611–612.
- (7) Lidy, W.; Sundermeyer, W. *Chem. Ber.* **1976**, *109*, 1491–1496.
- (8) Zeng, X.; Gerken, M.; Beckers, H.; Willner, H. *Inorg. Chem.* **2010**, *49*, 9694–9699.
- (9) Banert, K.; Berndt, C.; Hagedorn, M.; Liu, H. L.; Anacker, T.; Friedrich, J.; Rauhut, G. *Angew. Chem., Int. Ed.* **2012**, *51*, 4718–4721.
- (10) See, recent examples: (a) Kubicki, J.; Zhang, Y.; Vyas, S.; Burdzinski, G.; Luk, H. L.; Wang, J.; Xue, J.; Peng, H.-L.; Pritchina, E. A.; Sliwa, M.; Buntinx, G.; Gritsan, N. P.; Hadad, C. M.; Platz, M. S. *J. Am. Chem. Soc.* **2011**, *133*, 9751–9761. (b) Zeng, X.; Beckers, H.; Willner, H.; Grote, D.; Sander, W. *Chem.—Eur. J.* **2011**, *17*, 3977–3984.
- (11) Erben, M. F.; Boese, R.; Willner, H.; Della Védova, C. O. *Eur. J. Org. Chem.* **2007**, *2007*, 4917–4926.
- (12) Gómez Castaño, J. A.; Romano, R. M.; Beckers, H.; Willner, H.; Della Védova, C. O. *Inorg. Chem.* **2012**, *51*, 2608–2615.
- (13) Barnes, A. J. In *Matrix Isolation Spectroscopy*; Barnes, A. J.; Orville-Thomas, W. J.; Müller, A.; Gauffrés, R., Eds.; NATO ASI, Series C; Reidel Publishing: Dordrecht, The Netherlands, 1981; Vol. 76.
- (14) Bodenbinder, M.; Ulic, S. E.; Willner, H. *J. Phys. Chem.* **1994**, *98*, 6441–6444.
- (15) Durig, J. R.; Guirgis, G. A.; Krutules, K. A. *J. Mol. Struct.* **1994**, *328*, 55–75.
- (16) Mack, H.-G.; Della Védova, C.; Willner, H. *J. Mol. Struct.* **1993**, *291*, 197–209.
- (17) Milligan, D. E.; Jacox, M. E.; Bass, A. M.; Comeford, J. J.; Mann, D. E. *J. Chem. Phys.* **1965**, *42*, 3187–3195.
- (18) Freedman, T. B.; Nixon, E. R. *J. Chem. Phys.* **1972**, *56*, 698–707.
- (19) Desikan, V.; Liu, Y.; Toscano, J. P.; Jenks, W. S. *J. Org. Chem.* **2008**, *73*, 4398–4414.
- (20) O'Neill, S. R.; Shreeve, J. N. M. *Inorg. Chem.* **1972**, *11*, 1629–1631.
- (21) Corley, R. S.; Cohen, S. G.; Simon, M. S.; Wolosinski, H. T. *J. Am. Chem. Soc.* **1956**, *78*, 2608–2610.
- (22) Gombler, W.; Willner, H. *J. Phys. E* **1987**, *20*, 1286.
- (23) Schnöckel, H. G.; Willner, H. *Infrared and Raman Spectroscopy, Methods and Applications*; 1994, pp 297.
- (24) Frisch, M. J.; et al. *Gaussian 03* 2004.
- (25) (a) Becke, A. D. *J. Chem. Phys.* **1993**, *98*, 5648–5652. (b) Lee, C.; Yang, W.; Parr, R. G. *Phys. Rev. B* **1988**, *37*, 785. (c) Perdew, J. P.; Burke, K.; Ernzerhof, M. *Phys. Rev. Lett.* **1996**, *77*, 3865–3688. (d) Perdew, J. P.; Burke, K.; Ernzerhof, M. *Phys. Rev. Lett.* **1997**, *78*, 1396.
- (26) (a) Montgomery, J. J. A.; Frisch, M. J.; Ochterski, J. W.; Petersson, G. A. *J. Chem. Phys.* **1999**, *110*, 2822–2827. (b) Montgomery, J. A.; Frisch, M. J.; Ochterski, J. W.; Petersson, G. A. *J. Chem. Phys.* **2000**, *112*, 6532–6542.